EASR

Engineering and Applied Science Research

https://www.tci-thaijo.org/index.php/easr/index

Published by the Faculty of Engineering, Khon Kaen University, Thailand

Temporal and spatial variability of tropospheric NO_2 columns retrieved from OMI satellite data and comparison with ground based information in Thailand

Pichnaree Lalitaporn*

Department of Environmental Engineering, Faculty of Engineering, Kasetsart University, Bangkok 10900, Thailand

Received February 2017
Accepted April 2017

Abstract

Eight-year's of satellite data were retrieved from the OMI satellite to investigate temporal and spatial variability of tropospheric NO_2 columns during 2008-2015 over 6 regions of Thailand. The highest level of NO_2 columns was observed in the central region followed by the eastern, northern, northeastern, and southern regions. Moderately increasing trends of NO_2 columns were detected ranging from 16.62% to 39.48% over 7 years (ref. year 2008). In the north and northeast, the maximum levels of NO_2 columns were revealed during the biomass burning period of January-April. In the central and eastern regions, the maximum levels were observed during wintertime, i.e., November-February. For the southern region, the west coast showed higher levels during November-April while the east coast showed elevated levels during May-October. Comparative analysis of seasonal patterns of OMI observations versus ground based information of NO_2 concentrations and emissions revealed that they were generally in good agreement, particularly in the northern, eastern, and central regions. The results show that relative humidity has an effect on the correlations between OMI data and emissions. Overall, the OMI observations were shown to be useful in tracking atmospheric levels and emission sources of NO_2, especially when ground based data are not available.

Keywords: Emission inventory, NO_2, OMI, Satellite, Thailand

1. Introduction

Nitrogen dioxide (NO_2) is a major air pollutant playing a key role in atmospheric chemistry. The significant sources of NO_2 are anthropogenic sources (fossil fuel combustion, fertilizer application, and biomass burning) and natural sources (soil emissions, wildfires, and lightning). Long term exposure to NO_2 can contribute to respiratory infections and may be fatal [1]. Additionally, NO_2 has been recognized as the main source of photochemical ozone (O_3) [2]. During the day, NO_2 may react with hydroxyl (OH) radicals and form nitric acid (HNO_3). The sources and sinks of NO_2 are distributed heterogeneously. Therefore, NO_2 observations with board spectrum temporal and spatial scales were considerable.

Satellite remote sensing of NO_2 in the atmosphere was developed over 20 years since the Global Ozone Monitoring Experiment (GOME) was begun in 1995. This was followed by the SCanning Imaging Absorption spectroMeter for Atmospheric CHartographY (SCIAMACHY) in 2000, the Ozone Monitoring Instrument (OMI) in 2004, and GOME-2 in 2006. The products of satellite measurements provide the amount of NO_2 in columns integrated over the troposphere as vertical column densities (VCDs) [3]. The validation of satellite NO_2 VCDs using *in situ* measurements was done by many researchers [4-6]. The results from these studies show that satellite-based and *in situ* measurements are in good agreement under certain conditions. Worldwide trends of NO_2 observed from satellites have also been investigated over the past decade [1, 7-8]. Richter et al. [3] reported substantial reductions in NO_2 levels over Europe and the USA, while greatly increasing trends were observed over the industrial areas of China. Some studies [6, 9] developed a method to infer ground-level NO_2 concentrations from satellite NO_2 VCDs data by incorporating vertical profiles of NO_2. Their results present good agreement between satellite-derived surface NO_2 concentrations and ground based measurements.

This study focused on the use of OMI data over Thailand. The country is divided into six regions (characterized by Thai Meteorological Department). These are the northern (N), northeastern (NE), central (C), eastern (E), southern/west-coast (SW), and southern/east-coast (SE) regions. In general, the ground based monitoring stations in Thailand are located in urban and suburban areas, while they are sparse in many other remote sites. The use of global-image satellite monitoring products would provide useful information for air quality studies in Thailand. This study presents spatial distribution and temporal variability of NO_2 VCDs retrieved from OMI over six regions from 2008-2015. The comparisons of seasonal cycles of OMI data along with ground based concentrations and emissions were performed to investigate the consistency between these parameters. The meteorological data were analyzed to explore the effect on the correlations of OMI data and emissions. Long-term

*Corresponding author.
Email address: fengprla@ku.ac.th
doi: 10.14456/easr.2017.35

trends of NO_2 levels derived from both satellite and ground based data were also assessed.

2. Materials and methods

2.1 Satellite retrieved data

Satellite-based NO_2 VCDs in the troposphere were derived from the DOMINO (Dutch OMI NO_2) product Version 2.0 from 2008-2015. The data were provided by the Royal Netherlands Meteorological Institute (KNMI) and are available on the website of Tropospheric Emission Monitoring Internet Service (TEMIS) (http://www.temis.nl). The OMI instrument aboard the NASA's EOS-Aura satellite was launched in July 2004 with an equator crossing time of 13:40–13:50 local time (LT) [10]. The OMI sensor measures direct and atmospheric backscattered sunlight in the ultraviolet-visible (UV–Vis) ranging between 270 and 500 nm [11]. The spatial resolution of the product is up to 24×13 km^2 (at nadir). More details of OMI NO_2 retrieval were provided by Boersma et al. [12].

2.2 Emission inventory

Nitrogen oxide (NO_x=NO+NO_2) emissions used in this study were derived from the MACCity inventory. The MACCity emissions dataset is a new extension of the Atmospheric Chemistry and Climate Model Intercomparison Project (ACCMIP) and the Representative Concentration Pathways (RCP8.5) emissions dataset as part of the Monitoring Atmospheric Composition and Climate (MACC) and CityZen EU projects. MACCity provides datasets for 1960–2010 of anthropogenic emissions (from 9 sectors: transportation, energy, industries, ships, residential, solvents, agriculture/agriculture waste, waste, and aviation), and 1960–2008 for the biomass burning emissions (from 2 sectors: savanna burning and forest fires) in terms of a gridded (spatial resolution of 0.5°×0.5°) monthly mean global sectoral emissions. The datasets of MACCity inventory can be downloaded from the Emissions of Atmospheric Compounds and Compilation of Ancillary Data (ECCAD) database. More information on the development of the MACCity inventory was presented by van der Werf et al., Lamarque et al., Granier et al., and Diehl et al. [13-16].

2.3 Ground monitoring data

Hourly ground based data for NO_2 concentrations and relative humidity (RH) were obtained from the Pollution Control Department (PCD), Thailand over 44 stations in six regions during the same period as satellite data (2008-2015). Chemiluminescence [17] was used as a reference method to collect NO_2 at all stations. The hourly ground based NO_2 and RH data were collected between 12:00 and 16:00 LT corresponding to the OMI overpass time (13:40 – 13:50 LT) and were averaged as monthly data for analysis using OMI NO_2 VCDs. Since an OMI NO_2 pixel is approximately 24×13 km^2 and PCD NO_2 and RH are point-based, comparison of satellite and ground based data is not straightforward. Grid boxes with a 1.25°×1.25° search radius around the PCD stations were set up for the comparison. The ground based data that fall within the same grid boxes were grouped and averaged to compare with the averaged satellite data within the same boxes. Figure 1 presents the locations of the six grid boxes and 44 PCD stations in six regions of Thailand. Details of the locations of grid boxes and PCD stations are summarized in Table 1.

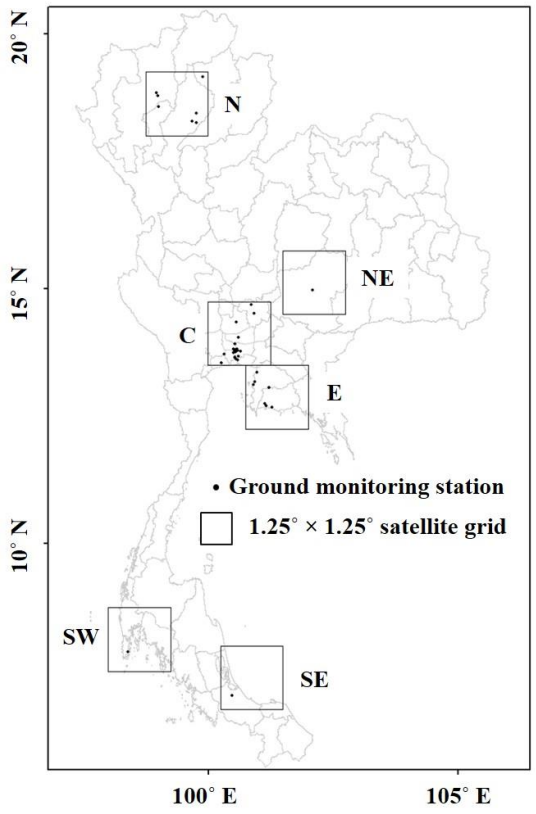

Figure 1 Locations of six grid boxes and 44 PCD stations in the six regions of Thailand

3. Results and discussion

3.1 Spatial and temporal variability of NO_2 VCDs

In order to analyze temporal and spatial variability of NO_2 levels over Thailand, eight years of data measuring monthly NO_2 VCDs were retrieved from OMI for the period of 2008-2015. Figure 2 presents the spatial and temporal variability of OMI NO_2 VCDs from January to December averaged from 2008-2015. The highest level of NO_2 VCDs can be observed in the central region where Bangkok, the capital city of Thailand, is located. Economic activities have enhanced the transportation and industrial sectors. These are the main contributors to high NO_2 levels in metropolitan Bangkok and surrounding areas. A similar result is presented by Ghude et al. [18] illustrating high levels of NO_2 VCDs in central Thailand from 2003-2006. High NO_2 VCDs were also detected around the Map Ta Phut Industrial Estate in the eastern region, where the main activities are petrochemical and related industries. Other hotspots can be seen in the north and northeast. Significant levels of NO_2 VCDs in these two regions were observed during biomass burning period of January-April with the highest peak in March. Forest fires and agricultural residue burnings of rice, maize and sugarcane are the major biomass burning activities during this period. This result correlates with the number of fire counts in an earlier study [19] showing higher number during February-April compared to other months in Chiang Mai province (northern Thailand) from 2010-2014. Figure 2 shows that the satellite instrument has the potential to be used as a tool for tracking atmospheric levels and major emission sources of NO_2, especially when ground based data are not available.

Table 1 Locations of the grid boxes and ground monitoring stations considered in this study

Region	Satellite Grid	Ground Monitoring Station			
	1.25°x1.25° Grid (Lat, Lon)	Station Name	City	Lat	Lon
N	18.00-19.25°N, 98.75-100.00°E	Knowledge Park	Phayao	19.16	99.90
		Chiangmai City Hall	Chiangmai	18.84	98.97
		Yupparaj Wittayalai School	Chiangmai	18.79	98.99
		Provincial Administrative Stadium	Lamphun	18.57	99.01
		Health Promotion Hospital Ta See	Lampang	18.44	99.77
		Provincial Waterworks Authority Mae Moh	Lampang	18.29	99.68
		Health Promotion Hospital Sob Pad	Lampang	18.25	99.77
NE	14.50-15.75°N, 101.50-102.75°E	Municipal Waste Water Pumping Station	Nakhon Ratchasima	14.98	102.09
C	13.50-14.75°N, 100.00-101.25°E	Na Phralan Police Station	Saraburi	14.69	100.87
		Khao Noi Fire Station	Saraburi	14.52	100.92
		Ayutthaya Witthayalai School	Ayutthaya	14.35	100.57
		Bangkok University Rangsit Campus	Pathum Thani	14.04	100.61
		Sukhothai Thammathirat Open University	Nonthaburi	13.91	100.54
		Electricity Generating Autority of Thailand (EGAT)	Nonthaburi	13.81	100.51
		Chandrakasem Rajabhat University	Bangkok	13.82	100.58
		Department of Land Transport	Bangkok	13.80	100.55
		Chokchai Police Station	Bangkok	13.79	100.60
		National Housing Authority Klongchan	Bangkok	13.78	100.65
		National Housing Stadium Huaykwang	Bangkok	13.78	100.57
		Ministry of Science and Technology	Bangkok	13.77	100.53
		National Housing Authority Dindaeng	Bangkok	13.76	100.55
		Roundabout 22 July	Bangkok	13.74	100.51
		Bansomdejchaopraya Rajabhat University	Bangkok	13.73	100.49
		Chulalongkorn Hospital	Bangkok	13.73	100.54
		Thonburi Power Sub-Station	Bangkok	13.73	100.47
		Nonsi Witthaya School,	Bangkok	13.71	100.55
		Mathayomwatsing School	Bangkok	13.68	100.45
		Ratburana Post Office	Bangkok	13.67	100.51
		Thai Meteorological Department Bangna	Bangkok	13.67	100.61
		Prabadng Rehabilitation Center	Samut Prakan	13.66	100.54
		Residence for Dept. of Mineral Resources	Samut Prakan	13.65	100.53
		South Bangkok Power Plant	Samut Prakan	13.62	100.56
		City Hall	Samut Prakan	13.61	100.60
		Highway District	Samut Sakhon	13.71	100.32
		Provincial Administrative Organization	Samut Sakhon	13.55	100.27
E	12.25-13.50°N, 100.75-102.00°E	Laem Chabang Municipal Stadium	Chonburi	13.12	100.91
		Sriracha Municipal Youth Center	Chonburi	13.17	100.93
		General Education Office	Chonburi	13.36	100.98
		Ta Sit Provincial Administrative	Rayong	13.06	101.22
		Health Promotion Hospital Maptaput	Rayong	12.71	101.17
		Agricultural Office	Rayong	12.67	101.28
		Field Crop Research Center	Rayong	12.74	101.14
SW	7.50-8.75°N, 98.00-99.25°E	Municipal Health Center	Phuket	7.88	98.39
SE	6.75-8.00°N, 100.25-101.50°E	Hat Yai Municipality	Songkhla	7.02	100.48

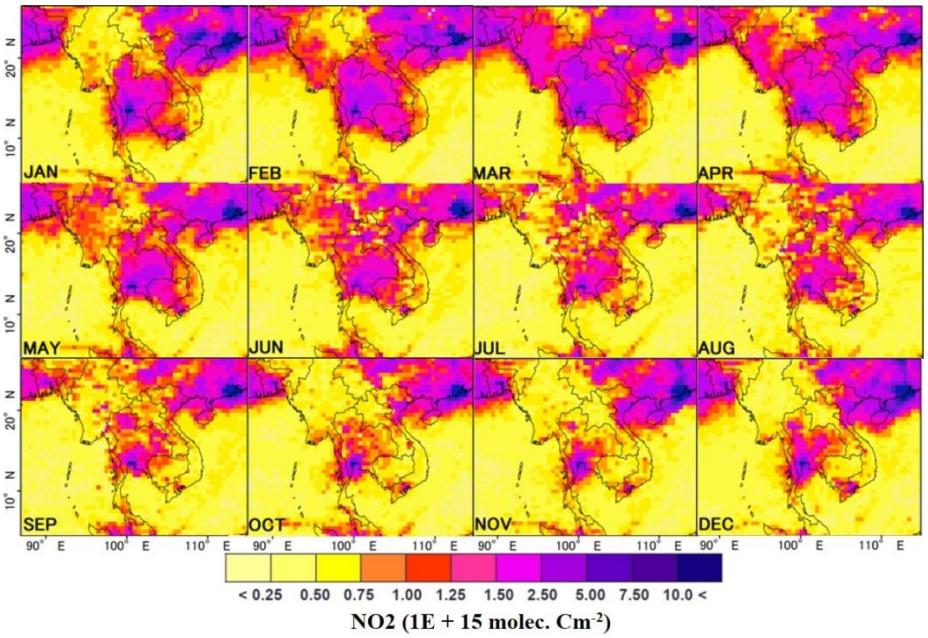

Figure 2 Spatial and temporal variability of OMI NO_2 VCDs from January to December averaged from 2008-2015

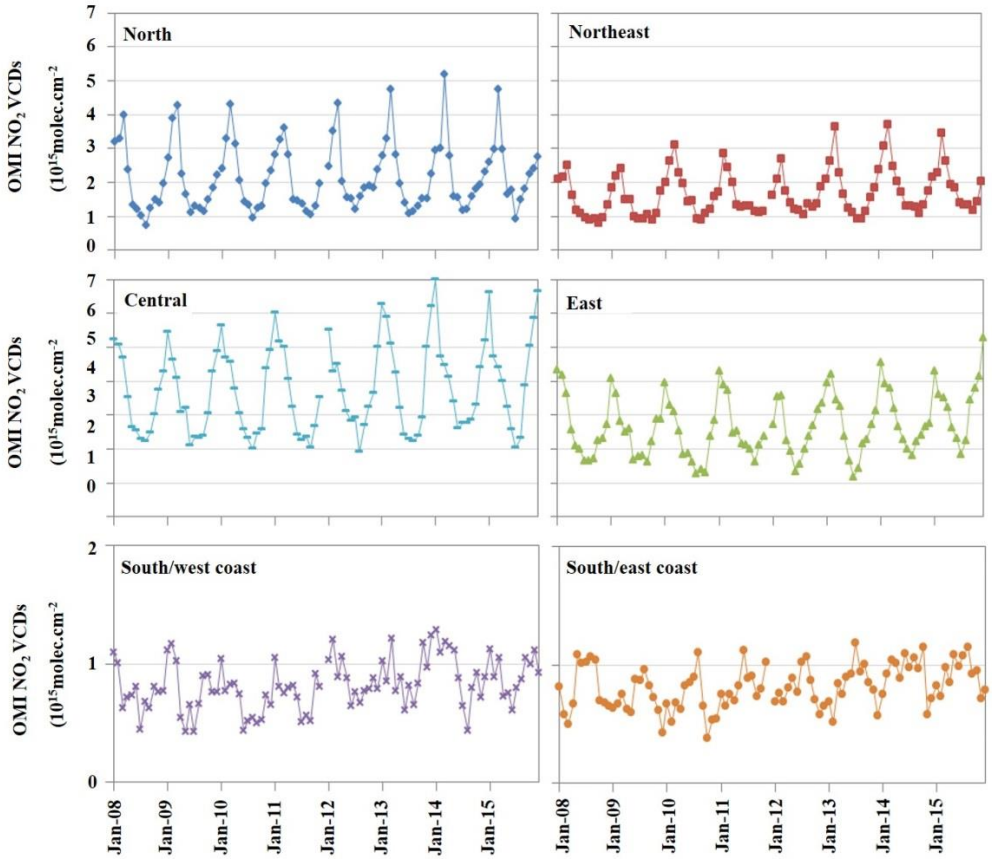

Figure 3 Time series of monthly OMI NO_2 VCDs from 2008-2015 over six regions of Thailand

Time series of OMI NO_2 VCDs in six regions extracted from the grid boxes (Figure 1) are presented in Figure 3 for the period of 2008-2015. In the north, high levels of NO_2 VCDs were observed from January-April, with the maximum in March. This is reflected in Figure 2. The minimum were commonly observed from July-August. Intensive biomass burning (forest fires and agricultural residue burnings) from January-April has been the major issue in the north for many years. This has contributed to high concentrations of several pollutants including NO_2. In the northeast, the seasonal pattern is quite similar to the northern region, where the maximum NO_2 VCDs appeared from January-April and the minimum occurred from July-November. For the central and eastern regions, the seasonal cycles showed the largest number of NO_2 VCDs in the wintertime (dry period) of November-March and the lowest number from June-September. In the south, the seasonal patterns of NO_2 VCDs both in the west and east coasts are not very clear. However, most of the peaks on the west coast were observed from October-March, whereas in the east coast the peaks were revealed in the period of May-September. Since the west and east coasts are separated by mountain ridges, the difference of the seasonal variation of NO_2 VCDs can be explained by the difference in meteorological condition on the two sides of the mountain range.

3.2 Comparison of satellite-based NO_2 and emissions

Monthly surface NO_x emissions from anthropogenic and biomass burning were obtained from the MACCity inventory over Thailand. The MACCity emissions from anthropogenic activities are available up to the year 2010 while data for biomass burning activities were gathered until 2008. For the years of 2009 and 2010, values of biomass burning emissions were assumed to be to the same as 2008. The sum of anthropogenic and biomass burning NO_x falling within the six grid boxes were compared with OMI NO_2 VCDs at the concurrent locations during 2008-2010. RH data were collected during the same period (averaged during 12:00-16:00 LT, 2008-2010) to investigate the relationship between MACCity NO_x emissions and NO_2 VCDs.

OMI data, MACCity emissions (the sum of anthropogenic and biomass burning NO_x), and RH were all normalized to the minimum values of each dataset and the average values compared for the period of January to December of 2008-2010 as illustrated in Figure 4. The results showed good agreement between OMI and MACCity data in the northern, northeastern, central, eastern, and southern/west coast regions with correlation coefficients (r) ranging from 0.89 to 0.99, as presented in Table 2. The comparisons between the RH values and OMI data also demonstrated that when the RH values were high, the NO_2 VCDs were low. The RH levels are commonly high during the rainy season. In general, with the presence of sunlight, water vapor will react with oxygen atoms (produced by photolysis of O_3) to form OH radicals. These in turn react with NO_2 to form HNO_3 ($NO_2 + OH \rightarrow HNO_3$) [20]. This process is the primary sink for NO_2 in the troposphere leading to a shorter lifetime for NO_2 and the lower levels of NO_2 VCDs. The correlation coefficients of the OMI data and RH levels are provided in Table 2. They ranged from -0.62 to -0.96. In the north and northeast, the MACCity NO_x emissions reached high levels during biomass burning period, January-April, in agreement with the OMI observations. Moreover, the RH levels during this time were

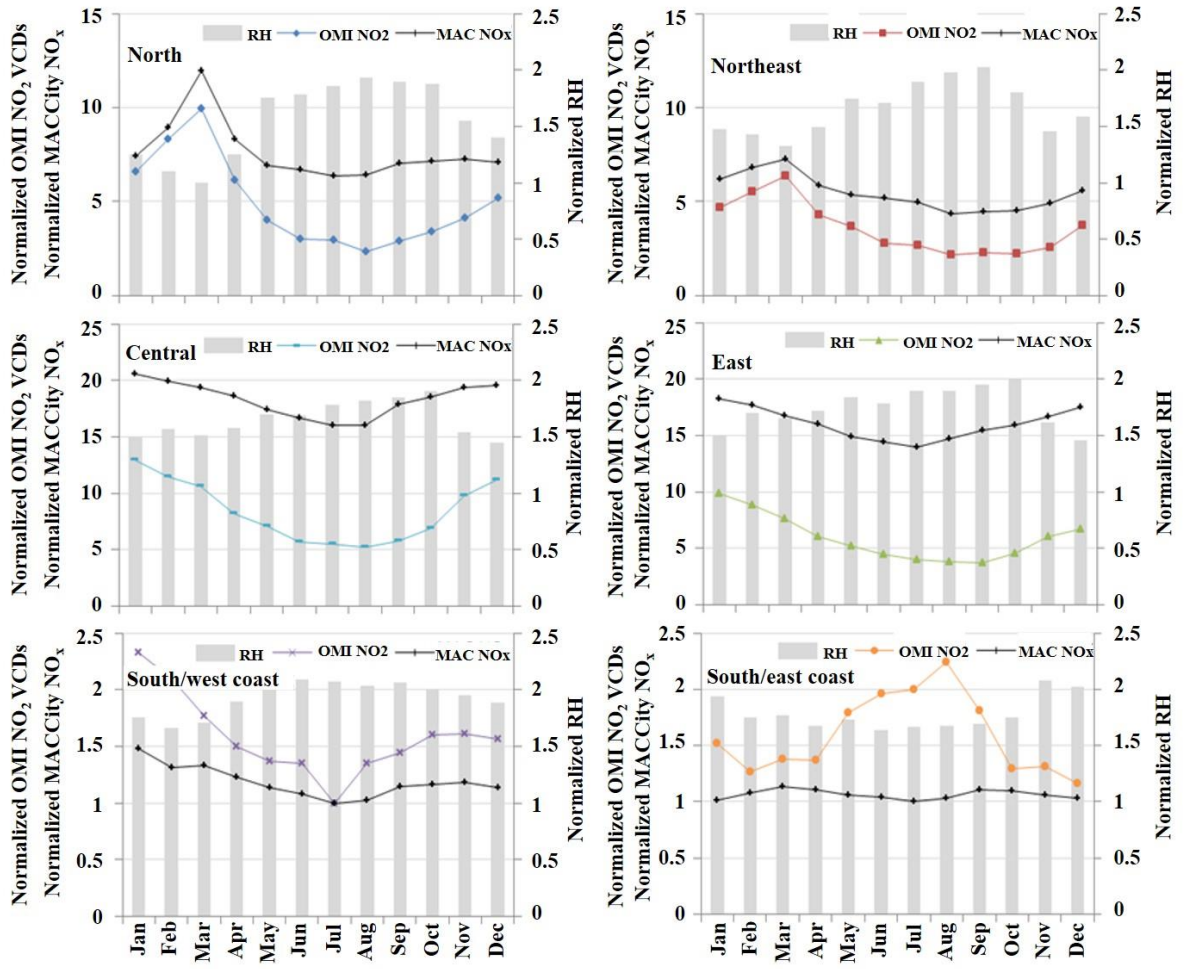

Figure 4 Monthly OMI NO_2 VCDs, MACCity NO_x emissions, and RH from January to December averaged for 2008-2010

Table 2 Correlation coefficients (r) of the relationship between OMI NO_2 VCDs and MACCity NO_x emissions (NO_2(O)-NO_x(M)), OMI NO_2 VCDs and RH (NO_2(O)-RH) and the averaged OMI NO_2 VCDs and MACCity NO_x emissions from 2008-2010

Region	r		Avg. data 2008-2010	
	NO_2(O)-NO_x(M)	NO_2(O)-RH	OMI NO_2 VCDs (10^{15}molec.cm^{-2})	MACCity NO_x (10^{-10}kgkm^{-2}s^{-1})
N	0.90	-0.96	2.06	1.25
NE	0.99	-0.81	1.51	0.89
C	0.93	-0.86	3.51	3.00
E	0.89	-0.78	2.48	2.62
SW	0.93	-0.84	0.73	0.19
SE	-0.40	-0.62	0.74	0.17

lower than in other months supporting the observation of more significant levels of NO_2 VCDs during these times. In the central and eastern regions, high levels of both NO_x emissions and NO_2 VCDs were present from November-March spanning the wintertime and dry periods (low RH) of Thailand. Since these two regions are the location of a city center and industrial estates, the main sources of NO_x emissions was from vehicles and factories. They consequently produce higher levels of NO_x during wintertime due to increased fuel combustion for heating [1].

For the west coast of the southern region, higher MACCity NO_x emissions were found during the dry period of October-March, which were also captured by OMI and reflected in higher levels of NO_2 VCDs during the same period. On the east coast, NO_x emissions were relatively constant throughout the year with slightly lower levels from November-February and June-August. However, OMI observed notably higher levels of NO_2 VCDs during June-August which contradicts the MACCity emission data resulting in low correlation between OMI and MACCity data (Table 2, r = -0.40). The reason for the discrepancy can be due to the lower RH levels from June-August causing a longer lifetime and higher levels of NO_2 in the troposphere. However, further study using an air quality model would lead to resolution of this issue. Table 2 also provides the average values of OMI NO_2 VCDs and MACCity NO_x emissions

from 2008-2010. Both datasets show the maximal levels in the central region followed by the eastern, northern, northeastern, and southern regions. This implies that OMI can be used to estimate NO_x emissions all over Thailand.

3.3 Comparison of satellite and ground based NO_2

To investigate the capability of OMI to measure ground based NO_2 levels, NO_2 VCDs and PCD NO_2 concentrations were compared. Figure 5 presents monthly cycles from January to December of the eight year averaged data from satellite and ground based NO_2 measurements from 2008-2015 over the six regions. Overall, OMI can be used to observe seasonal patterns of ground based NO_2 concentrations in all regions. The correlation coefficients of OMI and ground data are given in Table 3 and ranged from 0.62 to 0.98. Table 3 also provides averaged data from these two datasets during the study period. The highest 8-year averaged level of NO_2 VCDs was found in the central region (3.74×10^{15} molecules/cm^2) followed by the eastern, northern, northeastern, and southern regions. The highest averaged level of ground based NO_2 was in the northeastern region (18.84 ppb) followed by the central, southern/west coast, eastern, northern and southern/east coast regions.

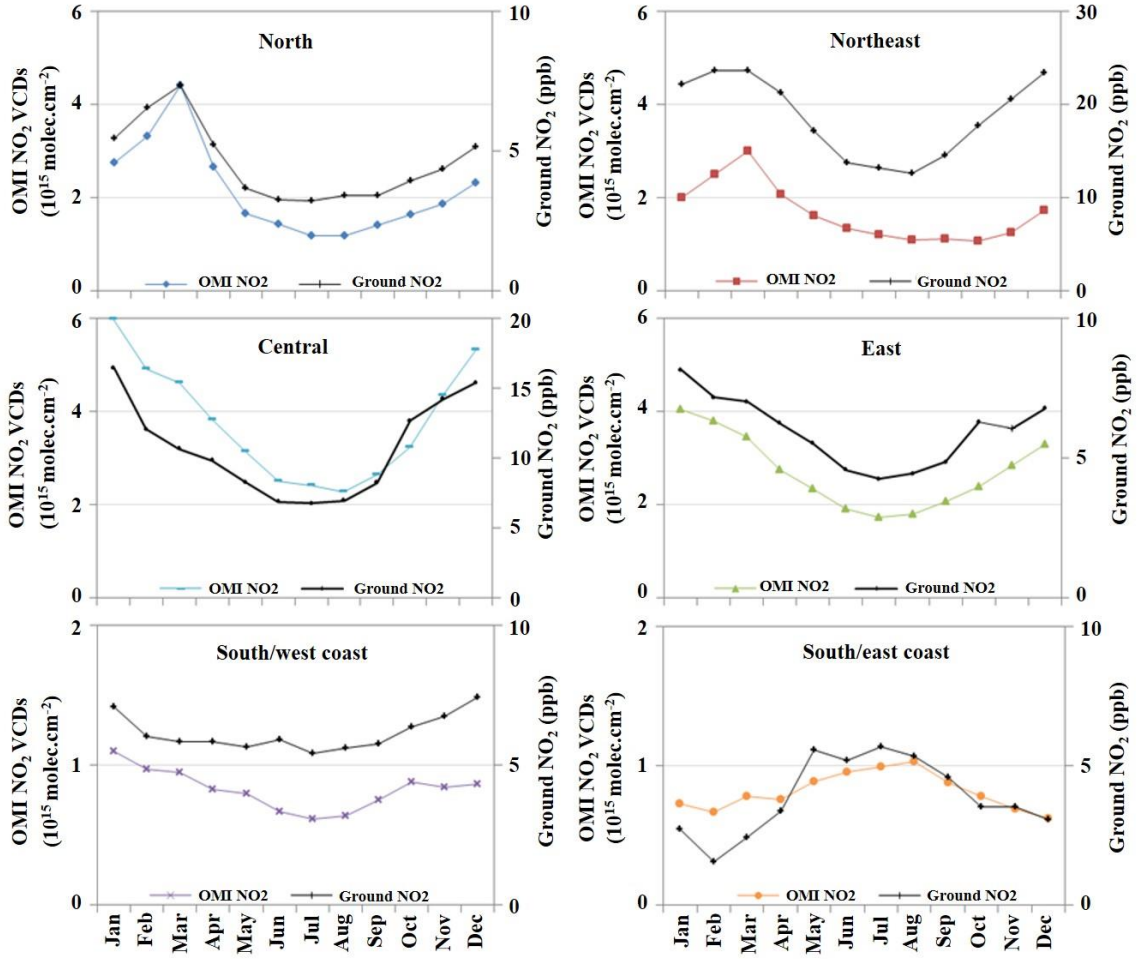

Figure 5 Monthly OMI NO_2 VCDs and ground based NO_2 concentrations from January to December averaged for the period of 2008-2015

Table 3 Averaged levels and trends of OMI NO_2 VCDs and ground based NO_2 concentrations during 2008-2015

Region	r	Avg. data 2008-2015		Trend (% per 7 years)	
	NO_2(O)-NO_2(G)	OMI NO_2 VCDs (10^{15}molec.cm^{-2})	Ground NO_2 conc. (ppb)	OMI NO_2 VCDs	Ground NO_2 conc.
N	0.98	2.15	4.59	16.62	20.66
NE	0.78	1.67	18.84	39.48	-
C	0.91	3.74	10.70	23.38	24.46
E	0.97	2.69	5.94	27.77	29.18
SW	0.60	0.81	6.14	30.99	61.96
SE	0.86	0.82	3.89	25.06	36.89

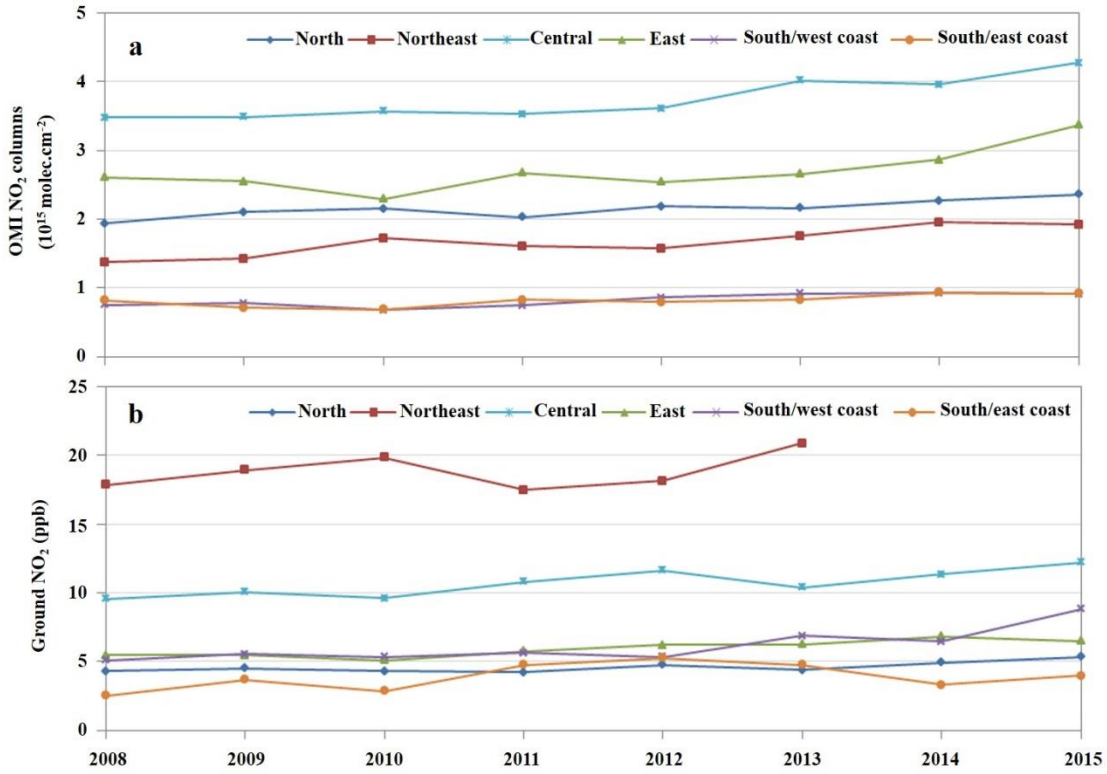

Figure 6 Trends of OMI NO_2 VCDs (a) and ground based NO_2 concentrations (b) for the period of 2008-2015

The reasons for the discrepancy between satellite and ground based datasets can be first explained by the production of NO_2 by lightning in the upper troposphere. Several studies [21-23] reported that lightning generally occurs more often in the tropics than in other parts of the world. PCD stations monitor NO_2 data at the Earth's surface while the satellite collects the data from the ground up to the satellite's sensor, lightning-produced NO_2 in the upper atmosphere can be monitored only by the satellite which in turn can introduces a discrepancy between these two datasets. Secondly, the ground based data in the northeast, the south/west coast, and the south/east coast were each derived from only one PCD station and compared with satellite-based data covering a 1.25°×1.25° box (Figure 1). This introduces more uncertainty. Furthermore, the ground based monitoring stations are commonly placed near the pollution hotspots whilst the satellite grids cover all the areas [24] and subsequently cause differences in the OMI and PCD datasets. These hypotheses are supported by the lower correlation coefficients of these three regions (r=0.62-0.86 in NE, SW, and SE) compared to the other three regions (r=0.91-0.98 in N, C, and E) where the ground based data were collected from many stations scattered within the 1.25°×1.25° boxes. Considering only the analysis in northern, eastern, and central Thailand, the results show that the maximum levels of the eight year averaged OMI and PCD data are both in the central region followed by the eastern and northern regions. This is the same trend revealed by comparative analysis of satellite data and MACCity emissions in a previous section.

Trend analysis of yearly NO_2 VCDs and ground based NO_2 concentrations over the six regions was performed and is presented in Figure 6 for the period of 2008-2015. The results in Table 3 reveal increasing trends in both datasets in all regions ranging from 16.62% to 39.44% for seven years of satellite based data and from 20.66% to 64.33% for seven years of ground based data. This does not include the northeastern region due to the unavailability of data for 2014 and 2015. Analysis of the northern, eastern, and central regions show that the highest increase of NO_2 VCDs was in the eastern region, followed by the central and northern regions. This agrees with the sequence of the trends seen in ground based NO_2 measurements.

4. Conclusions

The spatial and temporal variability of tropospheric NO_2 VCDs revealed by OMI was investigated over Thailand for the period of 2008-2015. The results showed that the maximum levels occurred in the central region, where the capital city of Thailand is located. In the central and eastern regions, higher levels were observed in the winter months of November-February. In the north and northeast, the highest levels were found during the biomass burning period of January-April. In the southern region, the west coast presented the maximum levels during November-April, while the east coast showed maximal levels from May-October. Comparative analysis of OMI data with MACCity NO_x emissions and RH showed that OMI can measure the seasonal patterns of NO_x emissions except on the south/east coast. This could be due to the effect of RH. However, further investigation using an air quality model would elucidate this issue. An eight year trend analysis revealed increasing levels in both OMI NO_2 VCDs and ground based NO_2 concentrations during the study period. Overall, the results in this study suggest that integrating OMI based and ground based measurements can provide valuable data to study spatial distribution and temporal variability in NO_2 levels, especially when ground based monitoring stations are not available. Further study of the NO_2 vertical profile will be useful to understand the relationship of satellite and

ground monitoring data and to develop a method for estimating ground level NO_2 concentrations derived from satellite NO_2 VCDs.

5. Acknowledgements

This research was supported by the Kasetsart University Research and Development Institute (KURDI). The data of OMI NO_2 VCDs are available through the TEMIS project website. Ground based monitoring data of NO_2 concentrations and relative humidity were obtained from PCD, Thailand. MACCity emission inventories were provided by ECCAD.

6. References

[1] van der A RJ, Eskes HJ, Boersma KF, van Noije TPC, Van Roozendael M, De Smedt I, et al. Trends, seasonal variability and dominant NO_x source derived from a ten year record of NO_2 measured from space. J Geophys Res. 2008;113(D04302):1-12.

[2] Valks P, Pinardi G, Richter A, Lambert JC, Hao N, Loyola D, et al. Operational total and tropospheric NO_2 column retrieval for GOME-2. Atmos Meas Tech. 2011;4(7):1491-514.

[3] Richter A, Burrows JP, Nüss H, Granier C, Niemeier U. Increase in tropospheric nitrogen dioxide over China observed from space. Nature. 2005;437(7055):129-32.

[4] Blond N, Boersma KF, Eskes HJ, van der A RJ, Van Roozendael M, De Smedt I, et al. Intercomparison of SCIAMACHY nitrogen dioxide observations, in situ measurements and air quality modeling results over Western Europe. J Geophys Res. 2007;112(D10311):1-20.

[5] Heland J, Schlager H, Richter A, Burrows JP. First comparison of tropospheric NO_2 column densities retrieved from GOME measurements and in situ aircraft profile measurements. Geophys Res Lett. 2002;29(20):1-4.

[6] Lamsal LN, Martin RV, van Donkelaar A, Celarier EA, Bucsela EJ, Boersma KF, et al. Indirect validation of tropospheric nitrogen dioxide retrieved from the OMI satellite instrument: Insight into the seasonal variation of nitrogen oxides at northern midlatitudes. J Geophys Res. 2010;115(D05302):1-15.

[7] Geddes JA, Martin RV, Boys BL, van Donkelaar A. Long-term trends worldwide in ambient NO_2 concentrations inferred from satellite observations. Environ Health Perspect. 2016;124(3):281-9.

[8] Lalitaporn P, Kurata G, Matsuoka Y, Thongboonchoo N, Surapipith V. Long-term analysis of NO_2, CO, and AOD seasonal variability using satellite observations over Asia and intercomparison with emission inventories and model. Air Qual Atmos Heal. 2013;6(4):655-72.

[9] Lamsal LN, Martin RV, van Donkelaar A, Steinbacher M, Celarier EA, Bucsela E, et al. Ground-level nitrogen dioxide concentrations inferred from the satellite-borne Ozone Monitoring Instrument. J Geophys Res. 2008;113(D16308):1-15.

[10] Boersma KF, Eskes HJ, Veefkind JP, Brinksma EJ, van der A RJ, Sneep M, et al. Near-real time retrieval of tropospheric NO_2 from OMI. Atmos Chem Phys. 2007;7(8):2103-18.

[11] Levelt P, van den Oord GHJ, Dobber MR, Malkki A, Stammes P, Lundell JOV, et al. The ozone monitoring instrument. IEEE Trans Geosci Remote Sens. 2006;44(5):1093-101.

[12] Boersma KF, Eskes HJ, Dirksen RJ, van der A RJ, Veefkind JP, Stammes P, et al. An improved tropospheric NO_2 column retrieval algorithm for the Ozone Monitoring Instrument. Atmos Meas Tech. 2011;4(9):1905-28.

[13] van der Werf GR, Randerson JT, Giglio L, Collatz GJ, Kasibhatla PS, Arellano AF. Interannual variability in global biomass burning emissions from 1997 to 2004. Atmos Chem Phys. 2006;6(11):3423-41.

[14] Lamarque J, Bond TC, Eyring V, Granier C, Heil A, Klimont Z, et al. Historical (1850–2000) gridded anthropogenic and biomass burning emissions of reactive gases and aerosols: methodology and application. Atmos Chem Phys. 2010;10(15):7017-39.

[15] Granier C, Bessagnet B, Bond T, D'Angiola A, van der Gon HD, Frost GJ, et al. Evolution of anthropogenic and biomass burning emissions of air pollutants at global and regional scales during the 1980–2010 period. Clim Change. 2011;109(1-2):163-90.

[16] Diehl T, Heil A, Chin M, Pan X, Streets D, Schultz M, et al. Anthropogenic, biomass burning, and volcanic emissions of black carbon, organic carbon, and SO_2 from 1980 to 2010 for hindcast model experiments. Atmos Chem Phys Discuss. 2012;12(9):24895-954.

[17] Fehsenfeld FC, Dickerson RR, Hübler G, Luke WT, Nunnermacker LJ, Williams EJ, et al. A ground-based intercomparison of NO, NO_x, and NO_y measurement techniques. J Geophys Res. 1987;92(D12):14710-22.

[18] Ghude SD, Van der A RJ, Beig G, Fadnavis S, Polade SD. Satellite derived trends in NO_2 over the major global hotspot regions during the past decade and their inter-comparison. Environ Pollut. 2009;157(6):1873-8.

[19] Punsompong P, Chantrara S. Pattern of biomass burning in Chiang Mai, Thailand and transportation of air pollutants in dry season. Proceedings of the 3rd EnvironmentAsia International Conference on Towards International Collaboration for an Environmentally Sustainable World; 2015 Jun 17-19; Bangkok, Thailand. Thai Society of Higher Education Institutes on Environment; 2015. p. 84-91.

[20] Stavrakou T, Müller JF, Boersma KF, Van Der A. RJ, Kurokawa J, Ohara T, et al. Key chemical NO_x sink uncertainties and how they influence top-down emissions of nitrogen oxides. Atmos Chem Phys. 2013;13(17):9057-82.

[21] Christian HJ, Blakeslee RJ, Boccippio DJ, Boeck WL, Buechler DE, Driscoll KT, et al. Global frequency and distribution of lightning as observed from space by the Optical Transient Detector. J Geophys Res. 2003;108(D1):1-15.

[22] Miyazaki K, Eskes HJ, Sudo K, Zhang C. Global lightning NO_x production estimated by an assimilation of multiple satellite data sets. Atmos Chem Phys. 2014;14(7):3277-305.

[23] Tie X, Chandra S, Ziemke JR, Granier C, Brasseur GP. Satellite measurements of tropospheric column O_3 and NO_2 in eastern and southeastern asia: Comparison with a global model (MOZART-2). J Atmos Chem. 2007;56(2):105-25.

[24] Hilboll A, Richter A, Burrows JP. Long-term changes of tropospheric NO_2 over megacities derived from multiple satellite instruments. Atmos Chem Phys. 2013;13(8):4145-69.